Photophysics of a 2,7-Dimethoxy-*N*-methylcarbazole-Based Polysiloxane

T. Ganguly,† L. Farmer, W. Li, J. Y. Bergeron, D. Gravel,* and G. Durocher*

Département de Chimie, Université de Montréal, C.P. 6128, Succ. A, Montréal, Québec H3C 3J7, Canada

Received July 6, 1992; Revised Manuscript Received December 15, 1992

ABSTRACT: The synthesis, characterization, spectroscopic properties, and photophysics of three poly(methylsiloxanes) (PMS) labeled with 2,7-dimethoxy-*N*-methylcarbazole (DMNMC) have been studied in dilute solutions both at room temperature and at 77 K. The chromophoric group has been attached to the polymeric chain through polymethylene spacers $(CH_2)_m$, where m = 3, 5, and 6. These polymers differ only in the nature of the spacer, and differential thermal analysis (DTA) has shown that the length of the spacer has a profound influence on the mesogenic properties of these liquid crystalline polymers. The degree of hypochromicity measured in the absorption spectra of these polymers in dilute solutions seems to be correlated to the mesogenic properties of the solid-state polymers as studied by DTA. Time-correlated single-photon-counting measurements were performed on these very dilute solutions of PMS. The decays are in all cases multiexponential at room temperature. This has been attributed to the existence of a distribution of conformations of preformed excimers with an associated spectrum of decay times. However, these traps (excimer sites) are at a relatively low level in dilute solution, making these polymers good candidates for photoconductivity study.

Introduction

Our research group has been involved lately in the development of organic photoconductive polymers (polysebacate and polysuccinic oligomers) containing alkylcarbazole–polynitrofluorene and –polynitrofluorenone bichromophores as pendant groups.[1-5] A correlation has been obtained between the xerographic gains of these bichromophores measured in photoactivity experiments and the rate constants for charge separation. The geminate charge recombination has also been studied quantitatively by picosecond flash photolysis since it is well-known that the key process affecting the overall photogeneration efficiency is the field-induced separation of carriers, competing with geminate recombination. It was shown that the rate for charge recombination in these systems is 3–4 orders of magnitude less than those for charge separation, which favors good electron transport in these media.[5]

We have found from these results that the mutual conformation of the chromophores has a great influence on the photoactivity of these oligomers. Our recent approach has been the design of a series of donor chromophores and D–A bichromophores based on the long axis of 2,7-disubstituted *N*-alkylcarbazoles used as pendant groups in polymethacrylate- and polysiloxane-based polymers. These systems give rise to liquid crystalline polymers which might possess improved photoconducting properties. Similar polymers have been reported by Strohriegl et al.[6] but the point of attachment of the carbazole mesogen is the nitrogen atom which is on the short axis of the molecule.

The influence that anisotropic properties of media like liquid crystals may exert on photophysical and photochemical processes is now recognized to be of enormous importance.[7] For mesogenic polymers or polymer liquid crystals (PLC), the intramolecular and intermolecular interactions between mesogenic moieties play the key role in determining the liquid crystalline properties. Earlier,

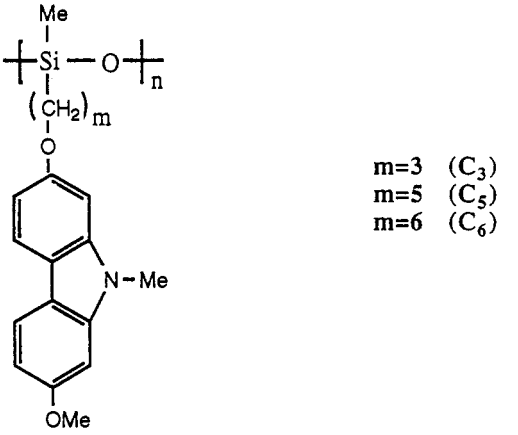

Figure 1. Molecular structures of the polymers C_3 (m = 3), C_5 (m = 5), and C_6 (m = 6).

changes occurring in the photophysical properties of PLC and LC both in the solid state and in solution with changes in concentration[8] and temperature were studied by steady-state[9] and time-resolved emission spectroscopy.[10] Polysiloxanes in particular have vast technological applications owing to their unique flexibility and stability. They have also been used in investigating the physics and structure of networks (ref 11 and references therein).

The photophysical properties of some 2,7-dimethoxycarbazoles in various environments were studied by steady-state and time-resolved fluorescence spectroscopy at room temperature[12] and at low temperature (77 K) in rigid glass matrices.[13] In a previous study[14] we reported the formation of physical dimers of these chromophores which explain the changes observed in the absorption and fluorescence spectra and also in excitation dynamics at high enough concentrations (>10^{-4} M) in tetrahydrofuran (THF).

We have chosen to pursue these studies using poly(methylsiloxanes) (PMS) labeled with 2,7-dimethoxy-*N*-methylcarbazole (DMNMC) connected along the long in-plane axis through some methylene spacers $(CH_2)_m$ of various lengths (m = 3, 5, and 6) as exemplified in Figure 1. The aim of this paper is to elucidate both the photophysical processes involved and also the effect of segmental motion and the constraints imposed by the polymer backbone.

* Authors to whom correspondence should be addressed.
† On leave from the Department of Spectroscopy, Indian Association for the Cultivation of Science, Jadavpur, Calcutta-700 032, India.

0024-9297/93/2226-2315$04.00/0

Scheme I

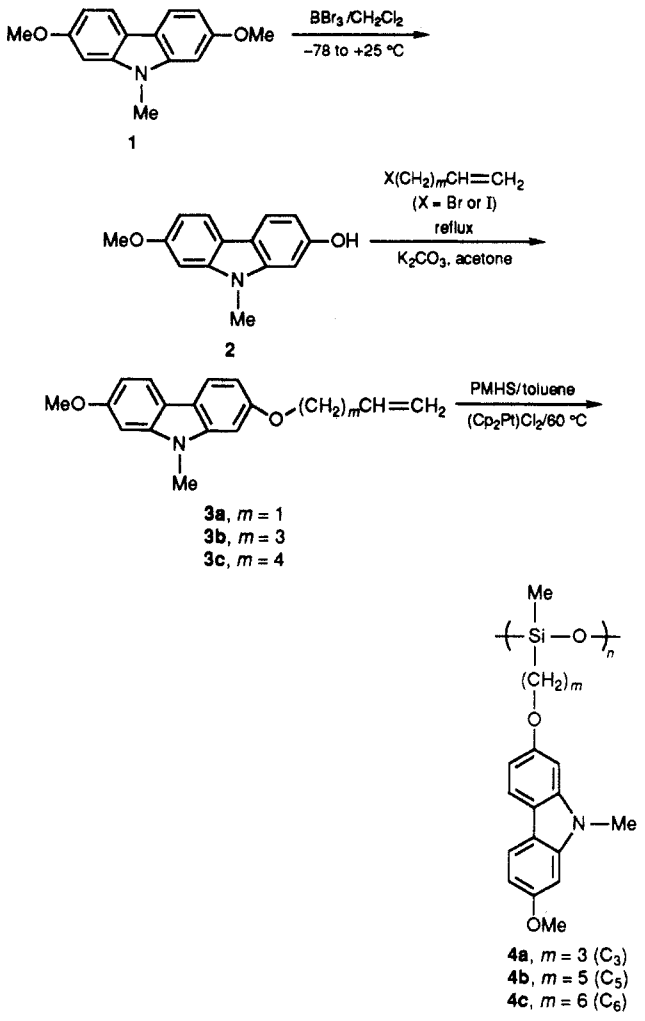

Experimental Section

Materials. Solvents, tetrahydrofuran (THF) of Omnisolv quality obtained from BDH and 2-methyltetrahydrofuran (2MTHF) purchased from Aldrich Chemical Co., were refluxed with $LiAlH_4$ for 2 h followed by distillation. Preparation of the carbazole derivatives and the polymers is illustrated in Scheme I and described below. All polymers were annealed before using them in the spectroscopic and the photophysical studies reported herein. They were heated at a fixed rate over their isotropic temperatures and cooled down to minimize heterogeneity.

Equipment. The UV absorption spectra were recorded on a PU8800 UV/vis spectrophotometer (Philips) using 1- and 5-cm quartz cells depending on the degree of dilution of the samples used. Corrected fluorescence and phosphorescence emission and excitation spectra were measured with a Spex Fluorolog Model 1902. Fluorescence decay and time-resolved measurements were performed with an Edinburgh Model 299 T multiplexed fluorimeter. Details on the instrument have been published elsewhere.[12] The instrument incorporates an all-metal coaxial hydrogen flashlamp which enables measurements of the decay components down to approximately 200 ps. Reconvolution analysis was performed by fitting over all the fluorescence decay including the rising edge. The kinetic interpretation of the goodness-of-fit was assessed using plots of weighted residuals, reduced χ^2 value, and the Durbin–Watson (DW) parameters.

The polarized fluorescence excitation and the polarized fluorescence and phosphorescence spectra were measured using an automated polarization design whose details have been given before.[13,15,16] For recording absorption and emission spectra at both 300 and 77 K, the concentration of the samples was varied from 1.5×10^{-5} to 1.5×10^{-6} mol dm^{-3}. All fluorescence lifetimes and steady-state measurements were carried out by using deaerated solutions made by the freeze–pump–thaw technique in five repeated cycles. The fluorescence quantum yields (ϕ_F) of the samples were measured relative to DMNMC in ethanol as standard ($\phi_F = 0.35$).[12]

All melting points were taken with a Büchi apparatus and are uncorrected. IR spectra were recorded on a Perkin-Elmer apparatus, Model 783, using the 1601-cm^{-1} band of polystyrene as reference. The ^{1}H NMR spectra were taken with a Varian VXR-300 instrument at 300 MHz in deuteriochloroform ($CDCl_3$) with Me_4Si as reference, unless otherwise indicated, and are reported in δ values. High-resolution mass spectra (EI) were recorded on an AEI MS-902 apparatus. Glass temperatures (T_g) were measured on a Perkin-Elmer Model DSC-4. Number-average molecular weights ($\bar{M}_n$) and weight-average molecular weights ($\bar{M}_w$) were determined by GPC on a Waters Model 510 apparatus using three Ultrastyragel columns in series, THF as eluant, and a Waters 410 differential refractometer, the calibration curve was that of polystyrene. The values are given in Table I. The elemental analyses were performed by Guelph Chemical Laboratories Ltd., Guelph, ON, Canada.

Differential thermal analysis (DTA) measurements were carried out using a Metler FP85 thermal analyzer under a N_2 atmosphere at 25 mL/min. The heating rate was 10 °C/min. DTA curves were recorded at second scan. Smectic and nematic mesophases were observed in C_5 only. C_3 exhibits a smectic mesophase together with C_6 even though the latter crystallizes at 80 °C. The transition temperatures are reproduced in Table I.

Synthesis and Characterization. (1) Preparation of the Carbazole Derivatives. *N*-Methyl-2-methoxy-7-hydroxycarbazole (2 in Scheme I). 2,7-Dimethoxycarbazole (1)[12,17] (5.0 g, 21 mmol) and 200 mL of dried dichloromethane were placed in a flame-purged 500-mL flask equipped with a septum. The mixture was stirred and cooled to −78 °C, and a 1 M solution of BBr_3 in CH_2Cl_2 (10 mL, 10 mmol) was added dropwise to the stirred solution. After the addition was complete, the mixture was stirred at room temperature for 2 h. The mixture was cooled to −78 °C again, and a 1 M solution of BBr_3 (10 mL, 10 mmol) was added dropwise to the stirred mixture. After the addition was finished, the mixture was stirred at 25 °C for 3 h, transferred into a separatory funnel, and extracted sequentially with water, 10% hydrochloric acid, ethyl acetate, and brine. The organic layer was dried and concentrated in vacuo to give crude material which was chromatographed on a silica gel column (40% AcOEt/hexane) to yield **2** (1.72 g, 36%) as white crystals: mp 164–166 °C; IR (KBr) 3410, 1625, 1491, 1235, 1131 cm^{-1}; ^{1}H NMR (DMSO-d_6) δ 9.37 (s, 1 H, O*H*), 7.78 (dd, J = 8.35 Hz, J = 3.57 Hz, 2 H, aromatic), 7.03 (d, J = 2.03 Hz, 2 H, aromatic), 6.81 (m, 2 H, aromatic), 3.84 (s, 3 H, OCH_3), 3.71 (s, 3 H, NCH_3); ^{13}C NMR (DMSO-d_6) δ 157.99, 156.14, 142.78, 142.31, 120.34, 119.98, 116.70, 115.34, 108.45, 107.33, 95.93, 93.75, 55.80 (OCH_3), 29.27 (NCH_3).

***N*-methyl-2-methoxy-7-((2-propenyl)oxy)carbazole (3a).** Under an inert atmosphere, a solution of **2** (2.0 g, 8.8 mmol), allyl bromide (1.491 g, 12.3 mmol), and potassium carbonate (1.946 g, 14.1 mmol) in spectrograde acetone (130 mL) was heated to reflux for 24 h. The mixture was cooled, transferred into a separatory funnel, and extracted sequentially with water, ether, and 10% sodium sulfate. The organic layer was then dried over anhydrous magnesium sulfate, filtered, and evaporated in vacuo to yield the crude product which was recrystallized from 95% ethanol to give **3a** (2.146 g, 90%) as white crystals: mp 96–98 °C; IR (KBr) 1605, 1475, 1210, 1105, 800 cm^{-1}; ^{1}H NMR ($CDCl_3$) δ 7.84 (d, J = 8.1 Hz, 2 H, aromatic), 6.84 (m, 4 H, aromatic), 6.14 (m, 1 H, CH_2=C*H*), 5.51 (dd, J = 15.7 Hz, J = 1.5 Hz, 1 H, CH_2=CH), 5.33 (dd, J = 9.1 Hz, J = 1.3 Hz, 1 H, CH_2=CH), 4.67 (d, J = 5.3 Hz, CH_2O), 3.90 (s, 3 H, OCH_3), 3.74 (s, 3 H, NCH_3); ^{13}C NMR ($CDCl_3$) δ 158.25, 157.16, 142.44, 142.33, 133.57, 120.01, 119.92, 117.41, 117.07, 116.85, 107.54, 106.90, 94.36, 93.14, 69.42, 55.64, 28.96.

***N*-Methyl-2-methoxy-7-((4-pentenyl)oxy)carbazole (3b).** Compound **3b** was prepared according to the procedure described above for the preparation of **3a**. The following quantities were used: **2** (2.5 g, 11 mmol), 5-iodo-1-pentene (3.235 g, 15.4 mmol), potassium carbonate (2.433 g, 17.6 mmol). The crude product, after standard workup, was chromatographed on silica gel (20% AcOEt/hexane) to give **3b** (3.05 g, 90%) as white crystals: mp 98–99 °C; IR (KBr) 1600, 1475, 1215, 1110, 800 cm^{-1}; ^{1}H NMR ($CDCl_3$) δ 7.85 (m, 2 H, aromatic), 6.84 (m, 4 H, aromatic), 5.90

Table I
Molecular Weights and Main Phase Transitions in These Poly(methylsiloxanes)

polymer	$\bar{M}_n$	$\bar{M}_w$	$\bar{M}_w/\bar{M}_n$	T_g (°C)	T_s[a] (°C)	T_n[b] (°C)	T_c[c] (°C)	T_m[d] (°C)
C_3	90 000	670 000	7.44	71	$T_g - 105$			105
C_5	123 000	631 000	5.11	62	$T_g - 100$	105–115		115
C_6	101 000	580 000	5.73	43			80	110

[a] Smectic domain. [b] Nematic domain. [c] Crystallization peak. [d] Melting point.

(m, 1 H, CH_2=C*H*), 5.08 (m, 2 H, C*H*$_2$=CH), 4.10 (t, J = 6.3 Hz, 2 H, C*H*$_2$O), 3.93 (s, 3 H, OC*H*$_3$), 3.75 (s, 3 H, NC*H*$_3$), 2.23 (q, J = 7.1 Hz, 2 H, C*H*$_2$), 1.96 (quintet, J = 7.0 Hz, 2 H, C*H*$_2$); ^{13}C NMR ($CDCl_3$) δ 158.18, 157.63, 142.39 (2 C), 137.85, 119.95, 119.92, 116.90, 116.84, 115.02, 107.44, 106.83, 94.01, 93.14, 67.71, 55.64, 30.13, 28.97, 28.58.

***N*-Methyl-2-methoxy-7-((5-hexenyl)oxy)carbazole (3c).** Compound **3c** was prepared in the same manner as **3b** by using the following quantities: **2** (2.50 g, 11 mmol), 6-iodo-1-hexene (3.235 g, 15.4 mmol), and potassium carbonate (2.433 g, 17.6 mmol). There was obtained, after standard workup and chromatography (20% AcOEt/hexane), 3.048 g (90%) of **3c** as white crystals: mp 99–100 °C; IR (KBr) 1600, 1465, 1215, 1110, 800 cm^{-1}; ^{1}H NMR ($CDCl_3$) δ 7.86 (m, 2 H, aromatic), 6.83 (m, 4 H, aromatic), 5.86 (m, 1 H, CH_2=C*H*), 4.98–5.01 (m, 2 H, C*H*$_2$=CH), 4.10 (t, J = 6.4 Hz, 2 H, OC*H*$_2$), 3.94 (s, 3 H, OC*H*$_3$), 3.74 (s, 3 H, NC*H*$_3$), 2.17 (q, J = 7.0 Hz, 2 H, C*H*$_2$), 1.88 (m, 2 H, C*H*$_2$), 1.67 (m, 2 H, C*H*$_2$); ^{13}C NMR ($CDCl_3$) δ 158.16, 157.66, 142.39 (2 C), 138.49, 119.19 (2 C), 116.91, 116.79, 114.59, 107.41, 106.82, 93.96, 93.13, 68.27, 55.63, 33.38, 28.94, 28.83, 25.35.

(2) Preparation of Polysiloxanes Bearing Pendant Carbazole Chromophores.[18] The polysiloxanes bearing pendant carbazole chromophores are prepared by a polyhydrosilylation reaction between poly(methylhydrogensiloxane) (PMHS) and an appropriate alkene. Platinum(II) such as dicyclopentadienylplatinum(II) chloride ([Cp_2Pt]Cl_2) is generally used as a catalyst in this reaction.

Poly[methyl(((*N*-methyl-2-methoxy-7-carbazolyl)oxy)propyl)siloxane] (4a). A mixture of **3a** (1.00 g, 3.7 mmol), PMHS (0.186 g, 3.1 mmol), and [Cp_2Pt]Cl_2 (1.6 mg) in 10 mL of dried, freshly distilled toluene was heated at 60–65 °C under argon until IR analysis showed that no absorption of Si–H at 2160 cm^{-1} remained (about 18–24 h). The polymer was then separated by precipitation into hexane and purified five times by precipitation from THF solution into hexane and dried in air to yield **4a** (0.755 g, 74%) as a light gray solid: T_g 71 °C; IR (KBr) 2930, 1610, 1465, 1254, 1215, 800 cm^{-1}; ^{1}H NMR ($CDCl_3$) δ 7.26–7.86 (m, 2 H, aromatic), 5.99–7.00 (m, 4 H, aromatic), 3.36–4.19 (m, 5 H, OC*H*$_2$, OC*H*$_3$), 2.46–3.23 (m, 3 H, NC*H*$_3$), 1.64–2.14 (m, 2 H, C*H*$_2$), 0.54–1.06 (m, 2 H, C*H*$_2$Si), 0.49–0.51 (m, 3 H, C*H*$_3$Si); ^{13}C NMR ($CDCl_3$) δ 157.83, 157.41, 141.97, 119.74, 119.53, 116.41, 116.32, 107.22, 106.85, 93.32, 92.548, 70.381, 55.268, 28.051, 23.209, 13.65, –0.241. Anal. Calcd for $(C_{18}H_{21}O_3NSi)_n$: C, 66.09; H, 6.47; N, 4.28; Si, 8.59. Found: C, 62.42; H, 6.32; N, 4.04; Si, 8.13.

Poly[methyl(((*N*-methyl-2-methoxy-7-carbazolyl)oxy)pentyl)siloxane] (4b). Polymer **4b** was prepared in the same manner as **4a** using the following quantities: **3b** (1.00 g, 3.4 mmol), PMHS (0.170 g, 2.8 mmol), and [Cp_2Pt]Cl_2 (1.6 mg). The crude product was precipitated five times from THF into hexane to give **4b** (0.801 g, 80%) as a gray solid: T_g 62 °C; IR (KBr) 2925, 1610, 1470, 1225, 1040, 810 cm^{-1}; ^{1}H NMR ($CDCl_3$) δ 7.51–7.70 (m, 2 H, aromatic), 6.36–6.76 (m, 4 H, aromatic), 3.51–3.99 (m, 5 H, OC*H*$_2$, OC*H*$_3$), 2.99–3.30 (m, 3 H, NC*H*$_3$), 1.65–1.82 (m, 2 H, C*H*$_2$), 1.39–1.65 (m, 4 H, C*H*$_2$C*H*$_2$), 0.60–0.66 (m, 2 H, C*H*$_2$Si), 0.086–0.18 (m, 3 H, C*H*$_3$Si); ^{13}C NMR ($CDCl_3$) δ 157.90, 157.51, 142.05, 141.99, 119.61, 119.49, 116.55, 116.44, 107.22, 106.79, 92.44, 92.67, 68.21, 55.32, 28.85, 29.42, 28.28, 23.12, 17.66, –0.179. Anal. Calcd for $(C_{20}H_{25}O_3NSi)_n$: C, 67.64; H, 7.10; N, 3.94; Si, 7.91. Found: C, 64.79; H, 6.79; N, 3.62; Si, 7.53.

Poly[methyl(((*N*-methyl-2-methoxy-7-carbazolyl)oxy)hexyl)siloxane] (4c). Polymer **4c** was prepared in the same manner as **4a** by using the following quantities: **3c** (0.980 g, 3.2 mmol), PMHS (0.159 g, 2.6 mmol), and [Cp_2Pt]Cl_2 (1.5 mg). The crude product was precipitated five times from THF into hexane to give **4c** (0.842 g, 86%) as a light gray solid: T_g 43 °C; IR (KBr) 2925, 1600, 1460, 1255, 1185, 1050, 785 cm^{-1}; ^{1}H NMR ($CDCl_3$) δ 7.36–8.01 (m, 2 H, aromatic), 6.53–6.82 (m, 4 H, aromatic),

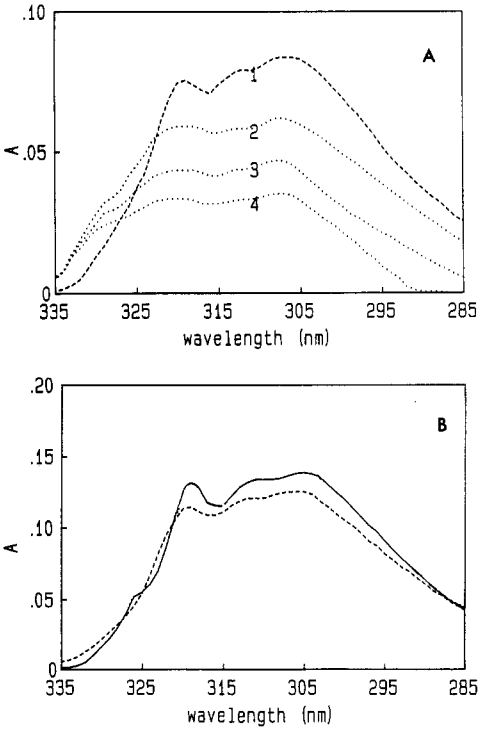

Figure 2. (A) Electronic absorption spectra in THF fluid solution at 296 K of (1) DMNMC, (2) C_5, (3) C_3, and (4) C_6. (Concentration of each sample is 1.5 × 10^{-6} mol dm^{-3} in a 1-cm square cell.) (B) Electronic absorption spectra of DMNMC at 296 K in (1) THF and (2) PMHS fluid solutions. (Concentration in each case is 1.5 × 10^{-6} mol dm^{-3} in a 1-cm square cell.)

3.64–4.06 (m, 5 H, OC*H*$_2$, OC*H*$_3$), 3.16–3.60 (m, 3 H, NC*H*$_3$), 1.64–1.80 (m, 2 H, C*H*$_2$), 1.17–1.64 (m, 6 H, C*H*$_2$C*H*$_2$C*H*$_2$), 0.44–0.78 (m, 2 H, C*H*$_2$Si), 0.096–0.36 (m, 3 H, C*H*$_3$Si); ^{13}C NMR ($CDCl_3$) δ 157.90, 157.51, 142.05, 141.99, 119.62, 119.49, 116.55, 116.44, 107.22, 106.79, 92.44, 92.67, 68.21, 55.33, 28.85, 29.42, 28.28, 23.12, 17.66, –0.48. Anal. Calcd for $(C_{21}H_{27}O_3NSi)_n$: C, 68.32; H, 7.37; N, 3.79; Si, 7.61. Found: C, 66.88; H, 7.10; N, 3.58; Si, 7.30.

Results and Analysis

Electronic Absorption Spectra. Figure 2A shows that the absorption spectrum of DMNMC in THF has approximately the same shape as that obtained in nonpolar solvents like 3-methylpentane (3MP)[12] except for the shoulder at 327 nm which is much less prominent in THF, but nevertheless more intense than in ethanol, reflecting the polarity of the solvent. This shoulder at 327 nm has previously been assigned to the (0–0) $^1L_b \leftarrow {}^1A$ electronic transition of DMNMC.[13] The photophysics of this molecule is complicated by two closely spaced excited states (^1L_a, ^1L_b) with varying amounts of charge-transfer character.[13] The region between 280 and 322 nm has been assigned to mainly $^1L_a \leftarrow {}^1A$.

However, when the chromophore DMNMC is attached to the PMS backbone through spacers of various lengths, its spectroscopic and photophysical properties appear to change remarkably. Figure 2A shows a strong hypochromic effect of the polymers compared to the free chromophore. When the chromophore (DMNMC) is dissolved in pure poly(methylhydrogensiloxane) (PMHS), the spec-

Table II
Changes Observed in the Spectroscopic and Photophysical Properties at 296 K of the Chromophore DMNMC When Dissolved in the Polysiloxane Environment and When Attached to the Polysiloxane Backbone through Some Spacers of Various Lengths as in the Cases of the Polymers C_3, C_5, and C_6 (Concentration of Each Sample in the Solvents Concerned Is $\sim 1.5 \times 10^{-6}$ mol dm^{-3})

sample	$\bar{\nu}_A$ (cm^{-1}) $^1B \leftarrow {}^1A$	$\bar{\nu}_A$ (cm^{-1}) $^1L_{a,b} \leftarrow {}^1A$	$\bar{\nu}_F^{max}$ (cm^{-1})[b]	$\langle\phi_F\rangle$[c] (±0.01)	$\langle\tau_F\rangle$[c] (ns) (±0.2)	$k_f \times 10^{-7}$ (s^{-1}) (±0.2)	$k_{nr} \times 10^{-7}$ (s^{-1}) (±0.2)	$k_f^{(t)} \times 10^{-7}$ (s^{-1}) (±0.2)
DMNMC	37 880	32 050[a]	27 930	0.40	8.2	4.9	7.4	15.0 (3.2)[d]
C_3	37 880	31 650[a]	27 700	0.08	6.3	1.3	15.0	6.5
C_5	37 880	31 650[a]	27 700	0.06	6.1	1.0	15.7	9.3
C_6	37 880	31 650[a]	27 700	0.04	6.0	0.7	16.8	4.9

[a] These measurements were done at the center of gravity of the absorption band, which is a mixture of $^1L_a \leftarrow {}^1A$ and $^1L_b \leftarrow {}^1A$ transitions.[12,13] [b] These values are taken from corrected fluorescence spectra. [c] Though in the cases of the polymer systems C_3, C_5, and C_6 more than one fluorescence lifetime is observed at room temperature (296 K), the average lifetime was calculated in each case to evaluate approximate values of k_f and k_{nr}. The ϕ_F values for the polymers also have to be considered as global values. [d] The value in parentheses is the value for the pure $^1L_b \leftarrow {}^1A$ transition in NMC.[12]

trum is approximately the same as that obtained in THF (Figure 2B). This excludes possible interactions between DMNMC and the polymer chain as a possible interpretation of the polymer spectra.

Similar hypochromy data have been reported on several aromatic polymers in liquid solutions[19] and more particularly on poly(vinylcarbazole (PVCA).[20] It was shown in PVCA that the oscillator strength of the $^1L_b \leftarrow {}^1A$ transition is reduced by 24% compared to that measured for *N*-ethylcarbazole. On the other hand, the oscillator strength of the $^1L_a \leftarrow {}^1A$ transition is more affected since it is reduced by 31%. Figure 2A shows quite clearly that a similar reduction is observed in these polysiloxanes and that C_6 is more affected than C_3 than C_5 in this order. Moreover, these spectra clearly indicate that the $^1L_b \leftarrow {}^1A$ transition (around 330 nm[13,14]) is less affected by the hypochromic effect than the $^1L_a \leftarrow {}^1A$ transition (mainly between 295 and 320 nm) as expected from earlier work.[19,20] The bands in the polymer spectra are also slightly shifted to the red following the interactions encountered by the chromophores (see Table II).

To explain the hypochromic effect in macromolecules, Vala and Rice have proposed the existence of helical regions.[21] This approach was sustained in the case of DNA, whose absorption strength returns to the normal value in helix-breaking solvents.[22] Moreover, a small hypochromic effect has indeed been measured in isotactic relative to atactic polystyrene by Vala and Rice.[21] However, this effect has not been observed in PVCA,[19,20] which prompted these authors to suggest that the tight packing of bulky aromatic side groups in wormlike chains, even without perfect ordering, should also be considered as a possible cause of the large hypochromic effects observed. Since hypochromism is a result of specific interactions between substituent groups and also between a group and the solvent in polymers, i.e., the interaction of each monomer transition moment with the surrounding dynamic and static fields, it is realistic to expect a strong effect of the polymethylene chain length on this spectroscopic behavior. It is interesting to point out here that polymers C_3 and C_5 have shown smectic phases (see Table I) but only C_5 has shown a nematic phase, where the chromophores are obviously less ordered than in smectic phases. Figure 2A shows that C_5 is less affected by hypochromicity compared to the others, and consequently one can conclude that the specific interactions between the DMNMC chromophores increase going from C_5 to C_3 to C_6 in THF.

It is well-known that the largest contribution to these specific interactions is from long-range dipole–dipole interaction of the band transition moments. Since DMNMC has also been shown to form dimers in highly concentrated (>10^{-4} M) solutions of THF,[14] one also has to discuss this possible cause of hypochromicity. It was clearly shown recently that when dimers are present, the band system of DMNMC is split into two components, each one showing isosbestic points, one at shorter wavelength (304 nm) and the other at longer wavelength (322 nm) than the absorption maximum.[14] The new absorption maxima are at 330 and 280 nm, which characterizes the two branches of the dimer. So the dimeric assumption cannot explain the hypochromic effect observed in the polysiloxanes since the effect observed here acts throughout the wavelength range of the absorption spectra (Figure 2A).

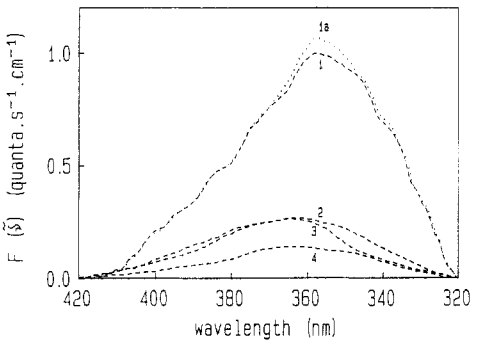

Figure 3. Room temperature (296 K) corrected fluorescence spectra (λ_{exc} = 305 nm) in THF fluid solution of (1) DMNMC, (2) C_5, (3) C_3, and (4) C_6. Curve 1a shows the room temperature corrected fluorescence spectra (λ_{exc} = 305 nm) of DMNMC in PMHS solvent. (Concentration in each case is 1.5×10^{-6} mol dm^{-3}.)

Fluorescence Spectra at 296 K. Figure 3 shows that the chromophores experience the same hypochromic effect in their fluorescence spectra as that observed in the absorption spectra and also similar red-shifted emissions in the polymers compared to solutions in THF or PMHS. However, it is worth pointing out here that the extent of quenching in any C polymer fluorescence intensity appears to be much greater than one could expect from the reduced absorption intensity. We have calculated and reported in Table II integrated fluorescence intensities which we called global fluorescence yields $\langle\phi_F\rangle$ (since the emission might come from various species) and integrated absorption spectra which we called also global theoretical radiative decays $k_f^{(t)}$. One can see that $\langle\phi_F\rangle$ is much more affected than $k_f^{(t)}$ when DMNMC is in a polymer environment, and the reason for that is the large increase in the nonradiative probability (k_{nr}) and also a decrease in the global observed radiative decay (k_f). Since k_f is more affected than $k_f^{(t)}$, one can conclude that the intermolecular interactions between the DMNMC chromophores in the polymers increase in the relaxed electronic excited state

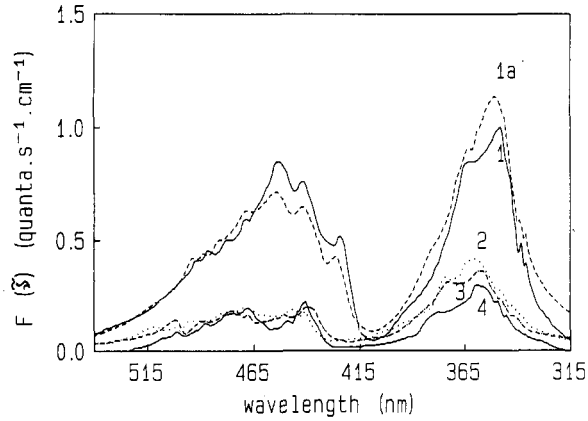

Figure 4. Corrected emission spectra at 77 K in a 2MTHF rigid glassy matrix (λ_{exc} = 305 nm) of (1) DMNMC, (2) C_6, (3) C_5, and (4) C_3. Curve 1a shows the low-temperature (77 K) emission spectra (λ_{exc} = 305 nm) of DMNMC in a PMHS rigid glassy matrix. (Concentration in each case is 1.5×10^{-6} mol dm^{-3}.)

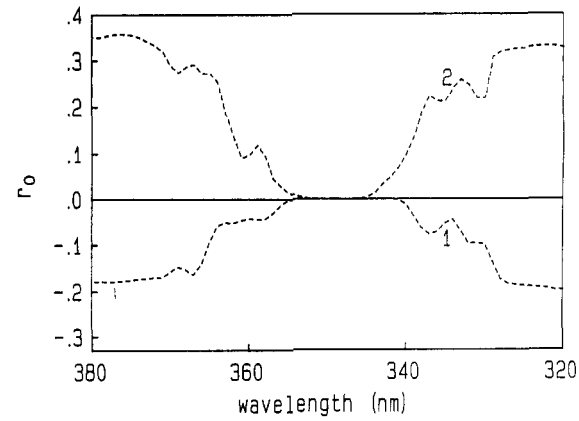

Figure 5. Fluorescence anisotropy (r_0) of C_3 in a 2MTHF rigid glassy matrix at 77 K at a concentration of 1.5×10^{-6} mol dm^{-3}: (1) λ_{exc} = 305 nm; (2) λ_{exc} = 320 nm.

responsible for the emission compared to the interactions effective in the ground electronic state. This might give rise to energy transfer, excitonic interactions, triplet–triplet annihilation, and excimeric traps throughout the polymer chain. Indeed, when one looks more carefully at those fluorescence spectra, an asymmetry is observed in the long-wavelength region in the polymer spectra. The intensity ratio I_{360}/I_{400} goes from 5 in the DMNMC spectra to 2.5 in the polymer spectra. In other words, some new species emit at longer wavelengths in the polymer spectra.

Since variation of the concentration of the polymers between 10^{-6} and 10^{-5} M did not modify the shape of these bands, intramolecular aggregates and/or excimer formation might be responsible for these fluorescence quenching results and the fluorescence band asymmetry observed. Two kinds of excimer have been characterized in poly(vinylcarbazole): the so-called "true excimer" or "low-energy excimer" or full overlap (sandwich) excimer or trap I excimer and the so-called second excimer or "high-energy excimer" or trap II excimer.[23] In the presence of some steric constraints in polymer systems, only trap II excimers could be expected.[24] That kind of excimer is situated at a slightly red-shifted position from the monomeric emission due to only partial overlap of the two moieties.

One way of distinguishing between the two traps is to measure the fluorescence spectra in low-temperature matrices. The trap I excimer is not observed but the trap II excimer is since it requires a very small activation energy.[25] Moreover, it is well-known that in order to observe such high-energy trap II fluorescence, energy transfer has to be involved from the randomly excited groups to the "trap II" sites. Only excitation hopping can explain this energy transfer. Fluorescence depolarization of the solid solutions then becomes a proof for the excitation hopping mechanism taking place.

Emission Spectra at 77 K. Low-temperature work in solid matrices of 2-methyltetrahydrofuran (2MTHF) has been performed on these systems. Figure 4 shows fluorescence spectra in the polymers that are vibrationally structured just like those of the free chromophores in 2MTHF or PMHS but shifted to the red by approximately 800 cm^{-1}. Nevertheless, the bandwidths of all fluorescence spectra in Figure 4 are similar, and the fluorescence intensity ratio I_{360}/I_{400} is the same in all spectra. Figure 5 also shows clearly that the fluorescence anisotropy of C_3 is similar to that of DMNMC in solid matrices.[13] Identical results are obtained for C_5 and C_6. Moreover, no triplet–triplet annihilation seems to take place since the ratio of fluorescence to phosphorescence intensities is kept constant when one compares the monomer and the polymer spectra. The last three experimental results tend to support the fact that no excitonic migration is taking place during the excited-state lifetime of DMNMC attached to the polymeric siloxane chain at 77 K. The trap II excimeric system is definitely not confirmed following these results. On the other hand, the extent of emission quenching and red shifts observed in the polymers compared to those in the free chromophore appears to be the same at both room and low temperatures. We also observed that the fluorescence excitation spectra of the polymers at 77 K exhibit a broad band at around 330 nm similar to those observed in the absorption spectra in THF at room temperature (see Figure 2A). The same hypochromicity as observed in the room temperature absorption and fluorescence spectra is also observed in the fluorescence and phosphorescence spectra at 77 K. The only spectral difference between the two temperatures is seen in the asymmetry of the room temperature fluorescence emission, which following the 77 K results above cannot be assigned to any sort of ground-state aggregation. The phosphorescence of the polymers is also red-shifted by about 800 cm^{-1} compared to the free chromophore in low-temperature matrices, and since this is much higher than the thermal energy ($\sim$54 cm^{-1}), one has to ascribe that to the different electronic environments felt by the side groups in the polymers.[20,23]

Accordingly, these overall steady-state results show the occurrence of some true or trap I excimer, though in low concentrations, in these polymeric systems at room temperature.

Time-Resolved Spectroscopic Measurements in the Nanosecond Domain. Figure 6 shows the fluorescence decay curves associated with the lamp profiles for C_3 in THF at room temperature (296 K). Similar results were obtained for all polymers studied here at various excitation and emission wavelengths. In all cases a three-exponential fit appears to give acceptable statistical parameters. Table III summarizes the results obtained. One should notice the absence of a measurable rise time of possible excimer formation. On the other hand, the isolated chromophore in THF or in polysiloxane solutions gives rise to only single-exponential decays as already observed in some other solvents.[12] This was interpreted at room temperature by the thermalization of the dual fluorescence emission which is only observed in low-temperature matrices. Semiempirical INDO/S-CI calculations coupled with solvatochromic shift theory have indeed shown the existence in DMNMC of a near-degeneracy of the ^1L_b and ^1L_a origins,

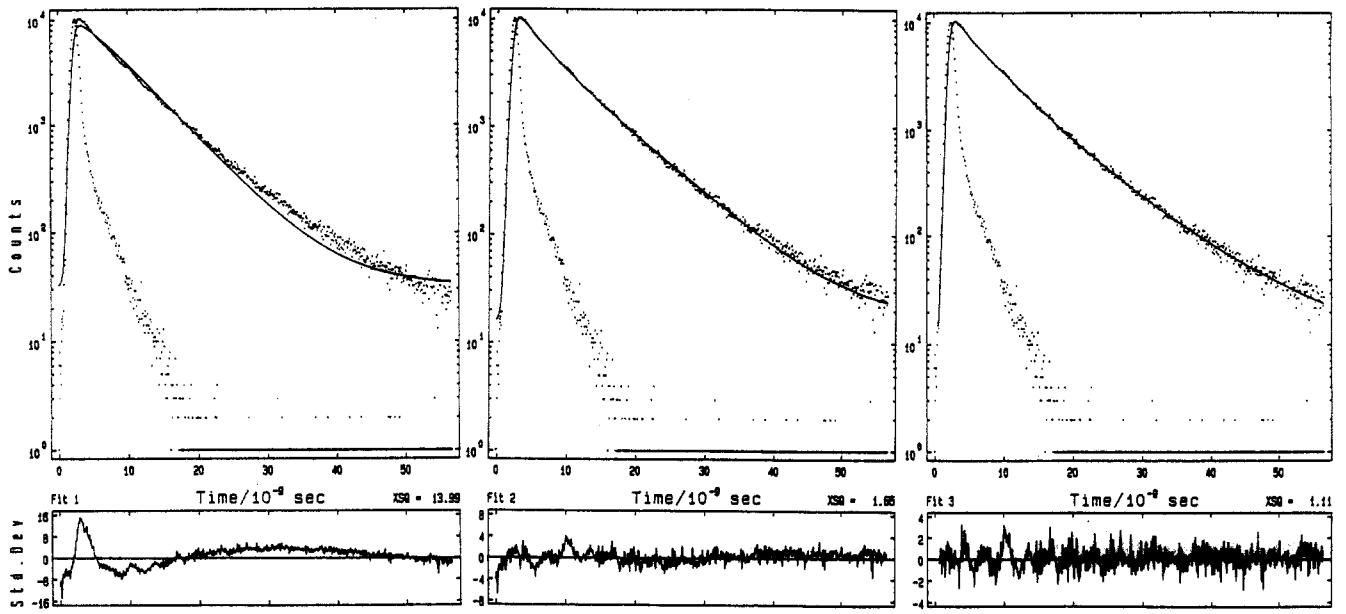

Figure 6. Fluorescence decay curves associated with the lamp profiles for C_3 polymer in THF fluid solution at a concentration of 1.5×10^{-6} mol dm^{-3} (λ_{exc} = 305 nm, λ_{em} = 350 nm). The curves from left to right show the single-, double-, and triple-exponential fit, residuals, and χ^2. The Durbin–Watson parameters are the following: for fit 1, DW = 1.42; for fit 2, DW = 1.50, for fit 3, DW = 1.83.

Table III
Fluorescence Decay Parameters at 296 K of the Chromophore DMNMC Alone When Dissolved in Polysiloxane and THF Fluid solution and When Attached to the Polysiloxane Backbone through Some Spacers of Various Lengths as in the Cases of the Polymers C_3, C_5, and C_6[a]

system	λ_{exc} (nm)	λ_{em} (nm)	τ_1[b] (ns) (±0.2)	τ_2[b] (ns) (±0.2)	τ_3[b] (ns) (±0.2)	B_1	B_2	B_3	$\langle\tau\rangle$[c] (ns) (±0.5)	f_1[d]	f_2	f_3	χ^2
DMNMC[e]	305	350	8.1										1.20
	320	350	8.0										1.19
DMNMC[f]	305	350	7.9										1.18
	320	350	8.0										1.24
C_3[e]	305[g]	350	1.6	7.0		0.44	0.56		6.2	0.16	0.84		1.11
	320	350	1.6	6.1	12.3	0.38	0.55	0.07	6.6	0.13	0.70	0.18	1.10
		390	1.8	5.2	11.2	0.28	0.62	0.10	6.2	0.10	0.66	0.24	1.10
	330	350	0.5	4.4	9.2	0.49	0.35	0.15	6.1	0.09	0.48	0.43	1.17
C_5[e]	305[g]	350	1.6	6.7		0.43	0.57		5.9	0.15	0.85		1.20
	320	350	1.0	4.7	9.1	0.37	0.44	0.19	6.2	0.10	0.49	0.41	1.11
		390	1.3	4.5	8.6	0.20	0.55	0.25	6.1	0.05	0.50	0.45	1.10
	330	350	0.5	4.0	8.6	0.46	0.35	0.19	6.0	0.08	0.43	0.49	1.18
C_6[e]	305[g]	350	2.0	7.0		0.50	0.50		5.8	0.23	0.77		1.09
	320	350	1.5	5.6	12.0	0.41	0.51	0.08	6.4	0.14	0.64	0.22	1.22
		390	1.5	5.6	12.0	0.38	0.53	0.09	6.5	0.13	0.64	0.23	1.18
	330	350	0.3	3.8	9.2	0.76	0.17	0.07	5.4	0.17	0.41	0.42	1.19

[a] The concentration of each sample in the solvents concerned is 1.5×10^{-6} mol dm^{-3}, B_1, B_2, and B_3 are the normalized preexponential factors, f_1, f_2, and f_3 are the fractional contributions of the various species to the steady-state spectra, and $\langle\tau\rangle$ is the average lifetime. [b] Obtained from the reconvolution fit: $A + B_1 \exp(-t/\tau_1) + B_2 \exp(-t/\tau_2) + B_3 \exp(-t/\tau_3)$. [c] Average lifetime calculated from the expression $\langle\tau\rangle = \sum_i B_i\tau_i^2/\sum_i B_i\tau_i$. [d] The fractional contribution of each species to the total fluorescence intensity is defined as $f_i(\lambda) = B_i\tau_i/\sum_i B_i\tau_i$. [e] In THF fluid solution. [f] In polysiloxane solution. [g] At this excitation wavelength a triple-exponential fit also gave the best statistics (χ^2 values and DW), but as the fractional contribution of τ_3 was very small, we neglected them.

which provides for very small regions of pure ^1L_b and ^1L_a absorption and fluorescence.[13]

Contrary to the room temperature decays, one can see in Table IV that practically only two exponentials become necessary to explain these decays in the polymers and also for DMNMC in polysiloxane and 2MTHF matrices at 77 K. Similar two-exponential decays have been obtained for DMNMC in low-temperature 3-methylpentane and ethanol matrices and were interpreted as a dual fluorescence arising from each state of the molecule, the longest lifetime being characteristic of the $^1L_b \rightarrow {}^1A$ transition and the shortest one characterizing the more allowed $^1L_a \rightarrow {}^1A$ transition.[13] The polymer composition does not seem to influence much the lifetimes of the chromophore, which is in accordance with the steady-state results obtained at 77 K. At some excitation and emission wavelengths though, the preexponential factors vary, giving rise to fractional contributions of each species which depend on these wavelengths much more than for the free chromophores in solid solutions. But even then, the average lifetime is practically constant if one takes into account the inherent error in the calculations. These lifetime results confirm that no energy transfer or excitonic migration is taking place during the lifetime of DMNMC attached to the polymeric siloxane backbone at 77 K.

The room temperature decays are more complex to interpret. The absence of a measurable rise time of excimer formation might indicate that the excimer conformation is preformed in these high molecular weight polymers and involves either a rapid reorientation of the fluorophore rather than segmental motion or rapid energy migration to excimer-forming sites. It is well accepted nowadays

Table IV
Fluorescence Decay Parameters for the Chromophore DMNMC Alone and the Polymer Systems C_3, C_5, and C_6 at 77 K in a 2MTHF Rigid Glassy Matrix (All Concentrations were 1.5×10^{-6} mol dm^{-3} at Room Temperature)

system	λ_{exc} (nm)	λ_{em} (nm)	τ_1[a] (ns) (±0.2)	τ_2[a] (ns) (±0.2)	τ_3[a] (ns) (±0.2)	B_1	B_2	B_3	$\langle\tau\rangle$ (ns) (±0.5)	f_1	f_2	f_3
DMNMC	305	335	0.26	6.1	10.6	0.24	0.23	0.53	9.6	0.01	0.20	0.79
		360		6.1	10.5		0.33	0.67	9.5		0.22	0.78
	328	335		6.2	11.0		0.34	0.66	9.9		0.23	0.77
		360		6.4	10.9		0.40	0.60	9.6		0.28	0.72
C_3	305	335		6.5	11.4		0.52	0.48	9.5		0.38	0.62
		360	0.4	6.3	11.8	0.14	0.45	0.41	9.7	0.01	0.37	0.63
	328	335		5.3	11.5		0.57	0.43	9.1		0.38	0.62
		360		5.6	11.2		0.44	0.56	9.6		0.28	0.72
C_5	305	335	0.9	5.3	10.8	0.34	0.34	0.32	8.5	0.05	0.33	0.62
		360	1.7	7.4	13.5	0.20	0.61	0.19	9.2	0.05	0.61	0.34
	328	335		5.1	10.6		0.51	0.49	8.8		0.33	0.67
		360		4.8	10.8		0.48	0.52	9.0		0.29	0.71
C_6	305	335		6.9	11.9		0.67	0.33	9.2		0.54	0.46
		360	0.5	6.4	12.1	0.35	0.40	0.25	9.2	0.03	0.45	0.52
	328	335		5.5	10.5		0.52	0.48	8.7		0.36	0.64
		360		5.4	11.0		0.46	0.54	9.4		0.29	0.71
DMNMC[b]	305	350	0.6	7.3	11.7	0.13	0.64	0.23	8.8	0.01	0.66	0.33
	328	335		7.2	12.1		0.71	0.29	9.2		0.59	0.41
		350	0.8	7.1	11.7	0.22	0.52	0.26	8.9	0.02	0.53	0.45

[a] Obtained from the reconvolution fit: $A + B_1 \exp(-t/\tau_1) + B_2 \exp(-t/\tau_2) + B_3 \exp(-t/\tau_3)$. [b] In a polysiloxane matrix at 77 K. In all the above measurements, χ^2 varies between 1.02 and 1.20.

that the excimer reaction kinetics in polymers do not generally obey the Birks scheme so that the intensity of monomer fluorescence ($I_M(t)$) which is normally described with two components requires the consideration of a third decay component:

$$I_M(t) = B_1 \exp(-t/\tau_1) + B_2 \exp(-t/\tau_2) + B_3 \exp(-t/\tau_3) \quad (1)$$

The third component has been previously explained by the evidence for isolated monomer sites which do not partake in the excimer-forming process (ref 26 and references therein). However, people realize that this model is oversimplistic in its approach. It is naive to assume that the complex distribution of chromophoric sites can be divided in only two groups. Another alternative explanation of the complex excimer behavior observed in polymer systems has been proposed in the form of eq 2:[27]

$$I_M(t) = B_1 \exp(-t/\tau_1) + B_2 \exp[-(t/\tau_2 + at^{1/2})] \quad (2)$$

This equation might be expected to apply when the close proximity of some fluorophores leads to a time-dependent rate of quenching analogous to that predicted by the Einstein–Smoluchowski diffusion theory. However, eq 2 does not fit our experimental results, giving rise to unacceptable large χ^2 values. This might be another proof of the fact that in these high molecular weight polymers, the excimers are preformed and independent of any lateral or rotational diffusion.

The kinetics might also be more complex here due to the fact that nearly isoenergetic electronic states in DMNMC are responsible for the fluorescence emission.[12,13] On close inspection, the data of Table III show that the average lifetime of the chromophore is reduced from 8 to 6 ns in the polymers at room temperature. Quenching is thus occurring probably due to energy migation to some trap I sites. One can conclude here that the length of the spacer group has no influence on the energy transfer probability in these polysiloxanes. This is opposite to the hypochromic effect observed in the absorption spectra where the ground-state interactions between the chromophores are dependent on the spacer groups that link DMNMC to the polymer backbone. Moreover, when one uses a three-exponential decay to explain an excimer kinetics, it is expected that the lifetimes of the various components will not vary with the emission wavelengths. This is what we observed here between 350 and 390 nm. However, the preexponential parameters are expected to vary in order to reflect the relative intensity of both monomer and excimer emissions. Small variations in the B parameters are observed but inside the experimental error. However, on the other hand, one can see that the preexponential factors B_2 and B_3 are much influenced by the excitation wavelengths. They can vary by as much as 20% and moreover these variations are complementary: when B_3 increases, B_2 decreases and vice versa.

This result strongly supports the assumption that τ_2 and τ_3 are the lifetimes of the ^1L_a and ^1L_b electronic states, respectively, in the polymeric environment. These lifetimes would then be associated to those obtained at 77 K. As far as τ_1 is concerned, Table III shows that it does not vary with the emission wavelength but it is strongly dependent upon the excitation wavelength, decreasing by a factor of at lesat 3 when the excitation is made in the $^1L_b \leftarrow {}^1A$ region of the absorption spectrum at 330 nm. This lifetime has to be assigned to a distribution of preformed excimer and/or aggregate conformations, each with differing overlap, molecular constraint, chromophore separation, and decay rate. The decay kinetics then becomes multiexponential. However, the experimental facts that this component is absent in the 77 K decays and its fractional contribution is practically independent of the spacer lengths provide evidences for various excimeric (trap I) conformations taking place at room temperature. Again here the length of the spacer group is not playing any role on the occurrence of these particular traps. Obviously these traps (the presence of more than one excimer emission) would also be expected to distort the kinetic analysis, leading to variations in the lifetimes of the original chromophore as a function of the excitation wavelength. Neither eq 1 nor eq 2 can be strictly applied in the study of such systems.

Since DTA of these polymers has shown the importance of the nature of the spacer group on the mesogenic properties of these polymers, investigations on neat polymer systems at different temperatures both by steady-state and time-resolved spectroscopic methods in the

nanosecond time domain are now underway and will be communicated shortly.

Concluding Remarks

Specific interactions of unknown nature but different from dimer formation between the DMNMC chromophores in their ground electronic states are responsible for the hypochromicity observed in the absorption, fluorescence, and phosphorescence spectra of these labeled poly(methylsiloxanes) (PMS). The $^1L_b \leftarrow {}^1A$ electronic transition is less affected by hypochromicity than the $^1L_a \leftarrow {}^1A$ transition as expected by their relative absorption dipole strengths. Moreover, the length of the spacer group between DMNMC and the polymer backbone seems to affect hypochromicity as it has also a profound influence on the mesogenic properties of these solid-state polymers. As pointed out recently on some other liquid crystalline polymers (PLC), it is very useful to study the solution properties of PLCs to obtain a better understanding of the intramolecular interactions between mesogenic moieties which together with the intermolecular interactions determine the liquid crystalline properties [28].

Both steady-state and time-resolved studies reveal that the photophysical properties of DMNMC change appreciably when connected with the PMS backbone through a polymethylene chain spacer in dilute solutions at room temperature. However, the length of the spacer does not influence much these photophysical properties, contrary to the influence it has on the absorption spectra. This shows that the species responsible for the complex decay kinetics are different from those responsible for the hypochromicity observed in the absorption spectra.

The multiexponential nature of the fluorescence decays of the polymers at room temperature shows these decays are much too complex to be described by either a kinetic model including isolated monomer sites or one which considers a time-dependent rate of quenching. This is due to the existence in each case of more than one and possibly a distribution of conformations of preformed excimers (involving a rapid reorientation of the chromophores, faster than 100 ps) with an associated spectrum of decay times. This fast reorientation mechanism is expected to be important in siloxanes according to conformational analysis which predicts very low torsional barriers, making it easy for the bonds to rotate, forming and dissociating the excimers.[29] However, these traps (excimer sites) are at a relatively low level at least in dilute solution, making these polymers good candidates for photoconductivity when sensitized with good electron acceptors.

Acknowledgment. We would like to acknowledge the Natural Sciences and Engineering Research Council of Canada and the Fonds FCAR (Québec) for support of this research. Bio-Mega Inc. is also gratefully acknowledged for fellowships to L.F.

References and Notes

(1) Brisse, F.; Durocher, G.; Gauthier, S.; Gravel, D.; Marqueès, R.; Vergelati, C.; Zelent, B. *J. Am. Chem. Soc.* **1986**, *108*, 6579.
(2) Zelent, B.; Messier, P.; Gravel, D.; Gauthier, S.; Durocher, G. *J. Photochem. Photobiol.* **1987**, *40*, 145.
(3) Zelent, B.; Messier, P.; Gauthier, S.; Gravel, D.; Durocher, G. *J. Photochem. Photobiol.* **1990**, *52*, 165.
(4) Gravel, D.; Gauthier, S.; Brisse, F.; Raymond, S.; D'Amboise, M.; Messier, P.; Zelent, B.; Durocher, G. *Can. J. Chem.* **1990**, *68*, 908.
(5) Ganguly, T.; Sharma, D. K.; Gauthier, S.; Gravel, D.; Durocher, G. *J. Phys. Chem.* **1992**, *96*, 3757.
(6) Domes, H.; Fisher, R.; Haarer, D.; Strohriegl, P. *Makromol. Chem.* **1989**, *190*, 165. Strohriegl, P. *Mol. Cryst. Liq. Cryst.* **1990**, *183*, 261. See also: Haarer, D.; Meyer, H.; Strohriegl, P. *Makromol. Chem.* **1991**, *192*, 617.
(7) Weiss, R. G.; He, Zh. *J. Am. Chem. Soc.* **1990**, *112*, 5535. Warkentin, M. S.; Leigh, W. J.; Jeffrey, K. R. *J. Am. Chem. Soc.* **1990**, *112*, 7329.
(8) Kurihara, S.; Ikada, T.; Tazuke, S. *Macromolecules* **1991**, *24*, 627.
(9) Subramaniam, R.; Patterson, L. K.; Levanon, H. *Chem. Phys. Lett.* **1982**, *93*, 578.
(10) Tamai, N.; Yamazaki, I.; Masuhara, H.; Mataga, N. *Chem. Phys. Lett.* **1984**, *104*, 485.
(11) Stein, A. D.; Hoffman, D. A.; Frank, C. W.; Fayer, M. D. *J. Chem. Phys.* **1992**, *96*, 3269.
(12) Zelent, B.; Ganguly, T.; Farmer, L.; Gravel, D.; Durocher, G. *J. Photochem. Photobiol. A* **1991**, *56*, 165.
(13) Ganguly, T.; Farmer, L.; Gravel, D.; Durocher, G. *J. Photochem. Photobiol. A* **1991**, *60*, 63.
(14) Ganguly, T.; Farmer, L.; Gravel, D.; Durocher, G. *Chem. Phys. Lett.* **1992**, *195*, 574.
(15) Zelent, B.; Harvey, P. D.; Durocher, G. *Can. J. Spectrosc.* **1984**, *29*, 23.
(16) Harvey, P. D.; Zelent, B.; Durocher, G. *Spectrosc. Int. J.* **1983**, *2*, 128; *Can. J. Spectrosc.* **1983**, *28*, 188; *Can. J. Spectrosc.* **1984**, *29*, 23.
(17) Hsieh, B. R.; Litt, H. *Macromolecules* **1986**, *19*, 516.
(18) Nestor, G.; White, M. S.; Gray, D. W.; Lacey, D.; Tayne, K. J. *Makromol. Chem.* **1987**, *188*, 2759. Percec, V.; Tomazos, D. *J. Polym. Sci., Part A* **1989**, *27*, 999.
(19) Okamoto, K.; Itaya, A.; Rusabayashi, S. *Chem. Lett.* **1974**, 1164; *Bull. Chem. Soc. Jpn.* **1976**, *49*, 2037; *Bull. Chem. Soc. Jpn.* **1976**, *49*, 2082.
(20) Klöpffer, W.; Rippen, G.; Kowal, J. *Makromol. Chem., Macromol. Symp.* **1986**, *5*, 187.
(21) Vala, M. T.; Rice, S. A. *J. Chem. Phys.* **1963**, *39*, 2348. Vala, M. T.; Haebig, J.; Rice, S. A. *J. Chem. Phys.* **1965**, *43*, 886.
(22) Thomas, R. *Biochim. Biophys. Acta* **1954**, *14*, 231.
(23) Klöpffer, W. In *Photophysics of Polymers*; Hoyle, C. E., Torkelson, J. M., Eds.; American Chemical Society: Washington, DC, 1987; Chapter 21.
(24) Ito, S.; Takami, T.; Tsujii, Y.; Yamamoto, M. *Macromolecules* **1990**, *23*, 2666.
(25) Johnson, G. E. *J. Chem. Phys.* **1975**, *62*, 4697.
(26) Soutar, I. *Polym. Int.* **1991**, *26*, 35.
(27) Fredrickson, G. H.; Frank, C. W. *Macromolecules* **1983**, *16*, 572.
(28) Kurihara, S.; Ikeda, T.; Tazuke, S. *Macromolecules* **1991**, *24*, 627.
(29) Rubio, A.; Freire, J. J.; Piérola, I. F.; Horta, A. *Macromolecules* **1989**, *22*, 4014.